

## Solvent Effects on the Conversion of Dicopper(II) $\mu\text{-}\eta^2\text{:}\eta^2\text{-Peroxo}$ to Bis- $\mu\text{-oxo}$ Dicopper(III) Complexes: Direct Probing of the Solvent Interaction

Hong-Chang Liang,<sup>†</sup> Mark J. Henson,<sup>‡</sup> Lanying Q. Hatcher,<sup>†</sup> Michael A. Vance,<sup>‡</sup> Christiana Xin Zhang,<sup>†</sup> David Lahti,<sup>§</sup> Susan Kaderli,<sup>§</sup> Roger D. Sommer,<sup>||</sup> Arnold L. Rheingold,<sup>||</sup> Andreas D. Zuberbühler,<sup>§</sup> Edward I. Solomon,<sup>‡</sup> and Kenneth D. Karlin<sup>\*†</sup>

Departments of Chemistry, The Johns Hopkins University, Baltimore, Maryland 21218, Stanford University, Stanford, California 94305, University of Basel, CH-4056 Basel, Switzerland, and University of Delaware, Newark, Delaware 19716

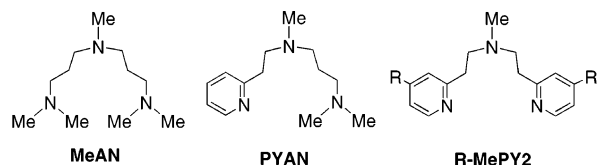
Received February 11, 2004

A new tridentate ligand, PYAN, is employed to investigate solvent influences for dioxygen reactivity with  $[\text{Cu}(\text{PYAN})(\text{MeCN})]\text{B}(\text{C}_6\text{F}_5)_4$  (**1**). Stopped-flow kinetic studies confirm that the adducts  $[\{\text{Cu}^{\text{II}}(\text{PYAN})_2(\text{O}_2)\}[\text{B}(\text{C}_6\text{F}_5)_4]_2$  ( $2^{\text{Peroxo}}$ ) and  $[\{\text{Cu}^{\text{III}}(\text{PYAN})_2(\text{O})_2\}[\text{B}(\text{C}_6\text{F}_5)_4]_2$  ( $2^{\text{Oxo}}$ ) are in rapid equilibrium. Thermodynamic parameters for the equilibrium between  $2^{\text{Peroxo}}$  and  $2^{\text{Oxo}}$  are as follows: THF,  $\Delta H^\circ \sim -15.7$  kJ/mol,  $\Delta S^\circ \sim -83$  J/K·mol; acetone,  $\Delta H^\circ \sim -15.8$  kJ/mol,  $\Delta S^\circ \sim -76$  J/K·mol. UV–visible absorption and resonance Raman spectroscopic signatures demonstrate that the equilibrium is highly solvent dependent; the mixture is mostly  $2^{\text{Peroxo}}$  in  $\text{CH}_2\text{Cl}_2$ , but there are significantly increasing quantities of  $2^{\text{Oxo}}$  along the series methylene chloride  $\rightarrow$  diethyl ether  $\rightarrow$  acetone  $\rightarrow$  tetrahydrofuran (THF). Copper(II)– $\text{N}_{\text{eq}}$  stretches (239, 243, 244, and 246  $\text{cm}^{-1}$  in  $\text{CH}_2\text{Cl}_2$ ,  $\text{Et}_2\text{O}$ , acetone, and THF, respectively) are identified for  $2^{\text{Peroxo}}$ , but they are not seen in  $2^{\text{Oxo}}$ , revealing for the first time direct evidence for solvent coordination in the more open  $2^{\text{Peroxo}}$  structure.

Previous studies on copper–dioxygen reactivity demonstrate that Cu(I) complexes with various tridentate<sup>1</sup> or bidentate<sup>2,3</sup> amine ligands can react with  $\text{O}_2$  to form both the  $\mu\text{-}\eta^2\text{:}\eta^2\text{-}$ (side-on)-peroxo dicopper(II) and/or the bis- $\mu\text{-oxo}$  dicopper(III) cores, and that these species can rapidly interconvert depending on reaction conditions.<sup>4–8</sup> In continu-

ing efforts to understand the factors that bias this equilibrium, we use UV–visible absorption and resonance Raman spectroscopic studies, as well as reaction kinetics analyses, to demonstrate the importance of solvent, and in particular to detect copper–solvent molecule binding.

Recently we reported on new Cu(I) complexes with ligands MeAN (see diagram) and AN,<sup>9</sup> which, differing by only one methyl group in their ligand structure (i.e.,  $-\text{CH}_3$  vs  $-\text{H}$ ), react with dioxygen in  $\text{CH}_2\text{Cl}_2$  to form disparate copper–dioxygen adducts, i.e., side-on peroxo or bis- $\mu\text{-oxo}$  species, respectively.<sup>10</sup> We also investigated the reactivity of a copper(I) complex with the ligand R-MePY2 (see diagram), where



ligand electronics (i.e.,  $-\text{R}$ ) strongly influence the side-on peroxo/bis- $\mu\text{-oxo}$  equilibrium.<sup>11</sup> Here, PYAN, a hybrid of MeAN and MePY2, is examined with respect to the dioxygen reactivity of its Cu(I) complex,  $[\text{Cu}^{\text{I}}(\text{PYAN})(\text{MeCN})]\text{B}(\text{C}_6\text{F}_5)_4$  (**1**), in a variety of solvents.

Complex **1** possesses a tetracoordinate copper(I) center with three N-donors from the PYAN ligand and a fourth

\* To whom correspondence should be addressed. E-mail: karlin@jhu.edu.

<sup>†</sup> The Johns Hopkins University.

<sup>‡</sup> Stanford University.

<sup>§</sup> University of Basel.

<sup>||</sup> University of Delaware.

- (1) Halfen, J. A.; Mahapatra, S.; Wilkinson, E. C.; Kaderli, S.; Young, V. G., Jr.; Que, L., Jr.; Zuberbühler, A. D.; Tolman, W. B. *Science* **1996**, *271*, 1397–1400.
- (2) Mahadevan, V.; Hou, Z.; Cole, A. P.; Root, D. E.; Lal, T. K.; Solomon, E. I.; Stack, T. D. P. *J. Am. Chem. Soc.* **1997**, *119*, 11996–11997.
- (3) Taki, M.; Teramae, S.; Nagatomo, S.; Tachi, Y.; Kitagawa, T.; Itoh, S.; Fukuzumi, S. *J. Am. Chem. Soc.* **2002**, *124*, 6367–6377.
- (4) Mirica, L. M.; Ottenwaelder, X.; Stack, T. D. P. *Chem. Rev.* **2004**, *104*, 1013–1045.

- (5) Que, L., Jr.; Tolman, W. B. *Angew. Chem., Int. Ed.* **2002**, *41*, 1114–1137.

- (6) Stack, T. D. P. *Dalton Trans.* **2003**, *10*, 1881–1889.

- (7) Cahoy, J.; Holland, P. L.; Tolman, W. B. *Inorg. Chem.* **1999**, *38*, 2161–2168.

- (8) Henson, M. J.; Mukherjee, P.; Root, D. E.; Stack, T. D. P.; Solomon, E. I. *J. Am. Chem. Soc.* **1999**, *121*, 10332–10345.

- (9) AN = 3,3'-Iminobis(*N,N*-dimethylpropylamine).

- (10) Liang, H. C.; Zhang, X. C.; Henson, M. J.; Sommer, R. D.; Hatwell, K. R.; Kaderli, S.; Zuberbühler, A. D.; Rheingold, A. L.; Solomon, E. I.; Karlin, K. D. *J. Am. Chem. Soc.* **2002**, *124*, 4170–4171.

- (11) Henson, M. J.; Vance, M. A.; Zhang, C. X.; Liang, H.-C.; Karlin, K. D.; Solomon, E. I. *J. Am. Chem. Soc.* **2003**, *125*, 5186–5192.

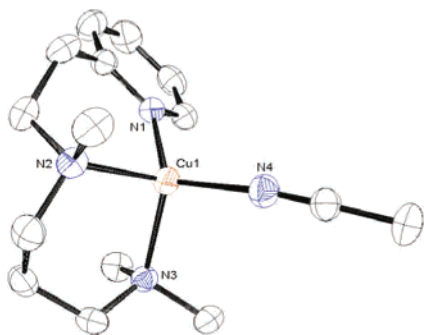


**Figure 1.** ORTEP diagram of the cationic portion of [Cu(PYAN)-(MeCN)]B(C<sub>6</sub>F<sub>5</sub>)<sub>4</sub>.

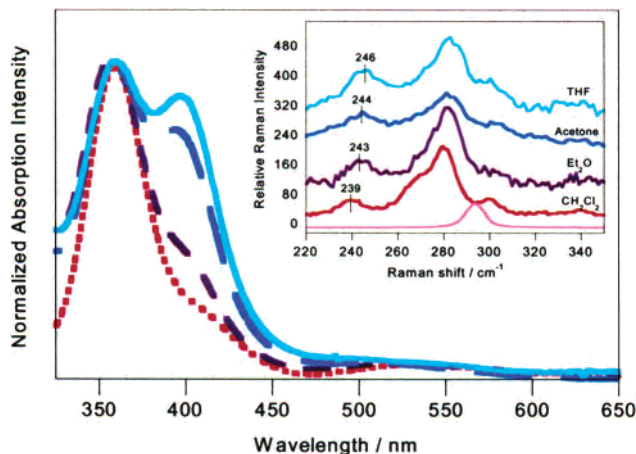


**Figure 2.** Absorption spectra of [Cu(PYAN)<sub>2</sub>O<sub>2</sub>]<sup>2+</sup> in CH<sub>2</sub>Cl<sub>2</sub> (red ···), diethyl ether (purple ---), acetone (blue ---), and THF (aqua —). Inset: rR spectra (λ<sub>ex</sub> = 363.8 nm) of [Cu(PYAN)<sub>2</sub>O<sub>2</sub>]<sup>2+</sup> in CH<sub>2</sub>Cl<sub>2</sub>, diethyl ether, acetone, and THF [Note: Solvent has been subtracted from the CH<sub>2</sub>Cl<sub>2</sub> trace. The scaled CH<sub>2</sub>Cl<sub>2</sub> spectrum is shown at bottom for comparison.]

N-donor from acetonitrile (Figure 1).<sup>12</sup> It reacts with O<sub>2</sub> to form varying quantities of side-on peroxo and bis-μ-oxo isomers, [Cu<sup>II</sup>(PYAN)<sub>2</sub>(O<sub>2</sub>)<sub>2</sub>]<sup>2+</sup> (**2<sup>Peroxo</sup>**) and [Cu<sup>III</sup>(PYAN)<sub>2</sub>(O)<sub>2</sub>]<sup>2+</sup> (**2<sup>Oxo</sup>**), respectively: the relative amount of each isomer is highly dependent on solvent (vide infra).<sup>1,7,10,13</sup> As seen by the UV–visible signatures associated with **2<sup>Peroxo</sup>** (360 nm) and **2<sup>Oxo</sup>** (400 nm),<sup>8</sup> **1** reacts with O<sub>2</sub> at –80 °C to form almost all **2<sup>Peroxo</sup>** in CH<sub>2</sub>Cl<sub>2</sub>. A greater proportion of the isomeric **2<sup>Oxo</sup>** forms in diethyl ether (Et<sub>2</sub>O) and acetone, while the highest ratio of **2<sup>Oxo</sup>** to **2<sup>Peroxo</sup>** (~1:1) forms in tetrahydrofuran (THF) (Figure 2). Resonance Raman (rR) studies confirm the conclusions from the UV–vis spectra:<sup>8,14</sup> excitation into the 360 nm band produces a characteristic side-on peroxo spectrum with ν(Cu···Cu) ~ 280 cm<sup>-1</sup> (Figure 2, inset) and ν(O–O) = 714 cm<sup>-1</sup> (Δ = –36),<sup>12,15</sup> while 400 nm excitation produces a characteristic dicopper(III) bis-μ-oxo spectrum, ν(Cu–O) = 585 cm<sup>-1</sup> (Δ = –25 cm<sup>-1</sup>).<sup>12</sup> Thus, the growth of the 400 nm absorption feature in the UV–vis spectra of **2** reflects a

### Scheme 1. Kinetic Model for the Oxygenation of **1**

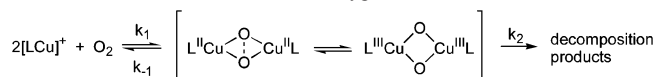


**Table 1.** Rate Constants (203 K) and Activation Parameters for the Processes in Scheme 1 in Various Solvents

parameter	acetone	THF	CH <sub>2</sub> Cl <sub>2</sub>
$k_1$ (M <sup>-2</sup> s <sup>-1</sup> )	$(1.50 \pm 0.02) \times 10^5$	$(4.2 \pm 0.1) \times 10^3$	$(2.10 \pm 0.03) \times 10^3$
$\Delta H_1^\ddagger$ (kJ/mol)	$-13.8 \pm 0.2$	$1.6 \pm 0.3$	$-5.1 \pm 0.3$
$\Delta S_1^\ddagger$ (J/K·mol)	$-211 \pm 1$	$-165 \pm 1$	$-203 \pm 1$
$k_{-1}$ (s <sup>-1</sup> )	$(5.0 \pm 0.8) \times 10^{-5}$	$(9.7 \pm 1.0) \times 10^{-5}$	$(1.1 \pm 0.1) \times 10^{-4}$
$\Delta H_{-1}^\ddagger$ (kJ/mol)	$66 \pm 1$	$60.5 \pm 0.9$	$55 \pm 1$
$\Delta S_{-1}^\ddagger$ (J/K·mol)	$-1 \pm 6$	$-21 \pm 4$	$-48 \pm 5$
$k_2$ (s <sup>-1</sup> )	$(7.7 \pm 0.1) \times 10^{-4}$	$(2.5 \pm 0.1) \times 10^{-4}$	<i>a</i>
$\Delta H_2^\ddagger$ (kJ/mol)	$39.9 \pm 0.3$	$46.6 \pm 0.5$	$86 \pm 6$
$\Delta S_2^\ddagger$ (J/K·mol)	$-105 \pm 1$	$-81 \pm 2$	$69 \pm 25$
$K_1$ (M <sup>-2</sup> ) <sup>b</sup>	$3.0 \times 10^9$	$4.3 \times 10^7$	$1.8 \times 10^7$
$\Delta H_1^\circ$ (kJ/mol)	$-79 \pm 1$	$-58.9 \pm 0.9$	$-60 \pm 1$
$\Delta S_1^\circ$ (J/K·mol)	$-209 \pm 6$	$-144 \pm 4$	$-155 \pm 5$

<sup>a</sup>  $k_2$  value uncertain due to photochemistry. <sup>b</sup> Calculated as  $k_1/k_{-1}$ .

significant shift in the equilibrium from **2<sup>Peroxo</sup>** toward **2<sup>Oxo</sup>** along the solvent series CH<sub>2</sub>Cl<sub>2</sub> → Et<sub>2</sub>O → acetone → THF.

To provide further insights, the stopped-flow kinetics of oxygenation of **1** were analyzed in CH<sub>2</sub>Cl<sub>2</sub>, acetone, and THF. The observed behavior conforms to the kinetic model shown in Scheme 1, confirming that the two Cu<sub>2</sub>–O<sub>2</sub> species are in rapid equilibrium as also seen in other systems.<sup>4,7,13</sup> In all solvents, oxygenation occurs with negative or very weakly positive activation enthalpies, indicative of an initial formation of the unstable superoxo complex, [Cu<sup>II</sup>(PYAN)-(O<sub>2</sub><sup>-</sup>)]<sup>+</sup> in a rapid left-lying preequilibrium, as previously observed in analogous copper complexes of tridentate amine ligand systems.<sup>10</sup> The enthalpic stability for the oxygenation reaction is considerably greater in acetone versus THF or CH<sub>2</sub>Cl<sub>2</sub> (Table 1). Also, the rate constant for the oxygenation of **1** in acetone is two orders of magnitude greater than the  $k_1$  in THF and in CH<sub>2</sub>Cl<sub>2</sub> (Table 1). A clear solvent effect is demonstrated, yet the reasons for the difference in rates are not understood at this time. Similar enhanced oxidation rates in acetone occur with the ligands AN<sup>9,10,16</sup> and H-MePY2.<sup>17,18</sup>

In THF and acetone, over the temperature range of 173 K to 263 K, the spectral changes reflecting the variation in relative amounts of **2<sup>Peroxo</sup>** and **2<sup>Oxo</sup>** allow for estimations of the thermodynamic parameters for the **2<sup>Peroxo</sup>** ⇌ **2<sup>Oxo</sup>** equilibrium. The parameters are identical within experimental uncertainty for the two solvents: THF,  $\Delta H^\circ \sim -15.7 \pm 0.4$  kJ/mol,  $\Delta S^\circ \sim -83 \pm 2$  J/K·mol; acetone,  $\Delta H^\circ \sim -15.8 \pm 1.2$  kJ/mol,  $\Delta S^\circ \sim -76 \pm 6$  J/K·mol.<sup>12</sup> These findings are in good agreement with literature values for related systems ( $\Delta H^\circ = -3.8$  kJ/mol·K,  $\Delta S^\circ = -25$  J/mol·K;<sup>7</sup>  $\Delta H^\circ \sim -2.5$  kJ/mol·K,  $\Delta S^\circ \sim -8.4$  J/mol·K<sup>13</sup>), reconfirming the very small barrier for peroxo/bis-μ-oxo isomerization.<sup>19</sup> The bis-μ-oxo dicopper(III) species is enthalpically but not

(12) See Supporting Information.

(13) Mahadevan, V.; Henson, M. J.; Solomon, E. I.; Stack, T. D. P. *J. Am. Chem. Soc.* **2000**, *122*, 10249–10250.

(14) Holland, P. L.; Cramer, C. J.; Wilkinson, E. C.; Mahapatra, S.; Rodgers, K. R.; Itoh, S.; Taki, M.; Fukuzumi, S.; Que, L., Jr.; Tolman, W. B. *J. Am. Chem. Soc.* **2000**, *122*, 792–802.

(15) To our knowledge, this is the second lowest known ν(O–O) in dicopper(II) side-on peroxo systems.

(16) Unpublished results for acetone.

(17) Obias, H. V.; Lin, Y.; Murthy, N. N.; Pidcock, E.; Solomon, E. I.; Ralle, M.; Blackburn, N. J.; Neuhold, Y.-M.; Zuberbuhler, A. D.; Karlin, K. D. *J. Am. Chem. Soc.* **1998**, *120*, 12960–12961.

(18) Liang, H.-C.; Karlin, K. D.; Dyson, R.; Kaderli, S.; Jung, B.; Zuberbuhler, A. D. *Inorg. Chem.* **2000**, *39*, 5884–5894.

(19) Cramer, C. J.; Smith, B. A.; Tolman, W. B. *J. Am. Chem. Soc.* **1996**, *118*, 11283–11287.

entropically favored relative to the side-on peroxo dicopper(II) isomer. The  $\text{Cu}_2(\text{O})_2$  enthalpic stabilization is most likely due to the stronger (and therefore more rigid)  $\text{Cu}^{\text{III}}$ –ligand bonds.

Further key insights come from rR spectroscopic data. Analysis of the low frequency region suggests that solvent directly interacts with the  $\text{Cu}_2\text{–O}_2$  core of  $2^{\text{Peroxoxo}}$  but not  $2^{\text{Oxo}}$ . Previous rR spectroscopic studies with proteins and model compounds support the assignment of the peaks attributed to the side-on peroxo dicopper(II) core: the intense peak at  $\sim 300\text{ cm}^{-1}$  represents the  $\text{Cu}\cdots\text{Cu}$  stretching mode, and the weaker satellites are N-equatorial ( $\text{N}_{\text{eq}}$ ) vibrations.<sup>20,21</sup> The spectrum of  $2^{\text{Peroxoxo}}$  exhibits vibrational features in  $\text{CH}_2\text{Cl}_2$  at 239, 278, and  $297\text{ cm}^{-1}$ , where the most intense feature at  $278\text{ cm}^{-1}$  corresponds to the  $\nu(\text{Cu}\cdots\text{Cu})$  mode. The satellite peak observed at  $239\text{ cm}^{-1}$  in  $\text{CH}_2\text{Cl}_2$  shifts to  $243\text{ cm}^{-1}$  in  $\text{Et}_2\text{O}$ , to  $244\text{ cm}^{-1}$  in acetone, and to  $246\text{ cm}^{-1}$  in THF (Figure 2, inset), significant shifts of  $4\text{–}7\text{ cm}^{-1}$  (out of  $\sim 240\text{ cm}^{-1}$ ). This pattern correlates with the solvent dependent shift of the equilibrium constant toward the bis- $\mu$ -oxo species  $2^{\text{Oxo}}$ , yet does not follow the trend in solvent dielectric constants, as previously reported.<sup>6,7</sup> In contrast, the rR feature at  $587\text{ cm}^{-1}$  associated with  $2^{\text{Oxo}}$  does *not* show a significant shift ( $\Delta = 2\text{ cm}^{-1}$ ) upon a change in solvent from  $\text{CH}_2\text{Cl}_2$  to THF.<sup>12</sup> Thus, despite the fact that the bis- $\mu$ -oxo feature is at much higher energy ( $590\text{ cm}^{-1}$  vs  $240\text{ cm}^{-1}$ ), its shift is negligible compared to the proportionally much larger  $7\text{ cm}^{-1}$  shift of  $2^{\text{Peroxoxo}}$  at  $\sim 240\text{ cm}^{-1}$ . These effects have been reproducibly observed in other systems.<sup>22</sup>

The UV–vis data imply that using solvents with greater coordinating ability shifts the equilibrium from  $2^{\text{Peroxoxo}}$  to  $2^{\text{Oxo}}$ . Following the same solvent trend, rR spectra show an increase in energy of the  $\text{Cu–N}_{\text{eq}}$  and  $\text{Cu}\cdots\text{Cu}$  vibrations of

the side-on peroxo complex, suggesting that the  $\text{N}_{\text{eq}}$  donors have moved more into the  $\text{CuN}_2\text{O}_2$  plane. The resulting greater in-plane orbital overlap would lead to strengthened  $\text{Cu–N}_{\text{eq}}$  and  $\text{Cu}_2\text{O}_2$  bonds. The negligible solvent dependent change in the rR spectra of  $2^{\text{Oxo}}$  indicates that this species is less susceptible to such solvent effects (e.g., axial coordination), which seems a reasonable presumption for a tight  $\text{Cu(III)–N}_2\text{O}_2$  core. However, overall thermodynamic considerations which favor  $2^{\text{Oxo}}$  require that these coordinating solvents effect an overall greater stabilization of the  $2^{\text{Oxo}}$  isomeric form; the nature of this interaction is not clear at this time.

In conclusion, the combined data demonstrate that solvent interaction and/or binding can be probed and plays a key role in the dynamic equilibrium between the side-on peroxo  $\text{Cu}^{\text{II}}_2\text{–}(\text{O})_2$  and bis- $\mu$ -oxo  $\text{Cu}^{\text{III}}_2\text{–}(\text{O})_2$  isomeric forms. We plan continued efforts to sort out the issues governing the formation, interconversion, and substrate reactivity tendencies of these copper–dioxygen adducts.

**Acknowledgment.** We thank Prof. T. D. P. Stack and co-workers for facilitating resonance Raman sample preparation at Stanford University. We are grateful to the National Institutes of Health (K.D.K., GM28962; E.I.S., DK31450) and Swiss National Science Foundation (A.D.Z.) for support of this research.

**Supporting Information Available:** Synthetic details, selected bond lengths and angles, kinetics (UV–vis traces and Eyring plots), resonance Raman, and X-ray crystallographic data (CIF). This material is available free of charge via the Internet at <http://pubs.acs.org>.

IC0498283

(20) Henson, M. J.; Mahadevan, V.; Stack, T. D. P.; Solomon, E. I. *Inorg Chem.* **2001**, *40*, 5068–5069.

(21) Solomon, E. I.; Tuczek, F.; Root, D. E.; Brown, C. A. *Chem. Rev.* **1994**, *94*, 827–856.

(22) Besides PYAN, this effect has been seen in the MeAN system (ref 10; see also Figure S4 in Supporting Information). Large shifts for the side-on peroxo but not bis- $\mu$ -oxo complexes have also been seen in other peroxo/oxo systems (Mahadevan, V.; Henson, M. J.; Stack, T. D. P.; Solomon, E. I. Unpublished results).